

Article

Irregularities in Meiotic Prophase I as Prerequisites for Reproductive Isolation in Experimental Hybrids Carrying Robertsonian Translocations

Oxana Kolomiets ¹, Irina Bakloushinskaya ^{2,*} , Mark Pankin ¹ , Valentina Tambovtseva ²
and Sergey Matveevsky ^{1,*} 

¹ Vavilov Institute of General Genetics, Russian Academy of Sciences, 119991 Moscow, Russia

² Koltzov Institute of Developmental Biology, Russian Academy of Sciences, 119334 Moscow, Russia

* Correspondence: i.bakloushinskaya@idbras.ru (I.B.); sergey8585@mail.ru (S.M.)

Abstract: The basic causes of postzygotic isolation can be elucidated if gametogenesis is studied, which is a drastically different process in males and females. As a step toward clarifying this problem, we obtained an experimental inbred lineage of the eastern mole vole *Ellobius tancrei*, whose founder animals were animals with identical diploid numbers $2n = 50$ but with different Robertsonian translocations (Rb), namely 2Rb4.12 and 2Rb9.13 in the female and 2Rb2.18 and 2Rb5.9 in the male. Here, we analyzed strictly inbred hybrids (F1, fertile and F10, sterile) using immunocytochemical methods in order to study spermatocytes during the meiotic prophase I. Previously, the presence of trivalents was assumed to have no significant effect on spermatogenesis and fertility in hybrids, but we demonstrated that spermatogenesis might be disturbed due to the cumulative effects of the retarded synapses of Rb bivalents as well as trivalents and their associations with XX sex bivalents. Alterations in the number of gametes due to the described processes led to a decrease in reproductive capacity up to sterility and can be examined as a mechanism for reproductive isolation, thus starting speciation.

Keywords: meiosis; gametogenesis; synapsis; synaptonemal complex; *Ellobius tancrei*; Mammalia; speciation



Citation: Kolomiets, O.; Bakloushinskaya, I.; Pankin, M.; Tambovtseva, V.; Matveevsky, S. Irregularities in Meiotic Prophase I as Prerequisites for Reproductive Isolation in Experimental Hybrids Carrying Robertsonian Translocations. *Diversity* **2023**, *15*, 364. <https://doi.org/10.3390/d15030364>

Academic Editors: Michael Wink, Luc Legal, Ben-Erik Van Wyk and Michel Baguette

Received: 29 December 2022

Revised: 27 February 2023

Accepted: 1 March 2023

Published: 2 March 2023



Copyright: © 2023 by the authors. Licensee MDPI, Basel, Switzerland. This article is an open access article distributed under the terms and conditions of the Creative Commons Attribution (CC BY) license (<https://creativecommons.org/licenses/by/4.0/>).

1. Introduction

Heredity and variability (“descent with modification” per Charles Darwin [1]) are the two basic phenomena behind speciation. Chromosomes, as carriers of genetic material, provide the precise inheritance of DNA. Through homologous recombination, genetic diversity increases. In the event of a deleterious mutation, a gametogenesis fail occurs, mainly in meiosis through the checkpoint systems that eliminate defective cells during certain meiotic stages [2,3]. This distinctive feature of speciation, in which divergence is ensured by chromosome mutations (changes in the structure and/or number of chromosomes), establishes postzygotic reproductive isolation due to the sterility or decreased fertility of hybrids [4]. Robertsonian (Rb) translocations, the most common chromosomal mutations in mammals, can persist in the natural population of many species [5–7]. The best-studied cases are house mice, common shrews, mole rats, and mole voles, though the human population’s inheritance of Rbs was also shown [8–17]. Rbs do not cause noticeable changes in chromatin, but they reshuffle it and, thus, change the linkage relationships.

A potential problem lies mainly with Rbs altering the number (lowering) and size (enlarging) of chromosomes, which, in turn, can disrupt the inner nuclear structure [18]. Moreover, in one study, when the chromosomal territories of fused chromosomes and their attachment sites to the nuclear envelope were located far from each other in the original nucleus, mutants, hybrids, and their backcrosses with the original form showed various kinds of disturbances [19]. In cases with numerous Rbs, heterozygous specimens demonstrate impaired meiotic development, mainly because of synapsis defects and the origin of

complex chains and rings [20–23]. For intra- and interspecies hybrids of mole voles, we previously described the formation of chains and stretched centromeres [23,24]. Some meiotic violations such as delayed synapsis, associations of autosomes with sex chromosomes, disturbed recombination, disjunction failure, and malsegregation of chromosomes might take place even when a single Rb chromosome emerges [25–27].

To study the possible postzygotic reproductive barriers due to the inheritance of chromosomal rearrangements, we chose an inbred line of the eastern mole vole *Ellobius tancrei*, which descended from a founder pair with the same diploid number, i.e., $2n = 50$, but with a different structure of double-armed chromosomes, namely the Robertsonian metacentrics (Rbs) 2Rb4.12 and 2Rb9.13 in the female and 2Rb2.18 and 2Rb5.9 in the male, as shown in Figure 1 [28,29]. Our experimental line was unique because we crossed strictly sibs in each generation. Here, we analyzed F10 males with distinct karyotypes. These males were crossed with females that had identical karyotypes. Thus, the genetic contribution of the females was constant, and, for the males, despite differences in the karyotype structure, the genetic background was similar due to the strictly inbred crosses. A large number of generations was possible because the F1 hybrids, both the males and females, were not sterile in the mole voles but demonstrated severely reduced fertility; this was in contrast to mice, in which males appeared to be sterile in some crosses [19,30]. The potential reason for this is the occurrence of sex chromosomes in *E. tancrei*, namely XX in males and females [31]. This system of isomorphic XX sex chromosomes is unusual for mammals but demonstrates specific behavior for females and males during the prophase I [32–34]. Karyotype diversity in our inbred line was observed starting from F2, and the diploid numbers changed to 48–52 with various sets of Rbs [35]. The rapid changes observed in the diploid number and the generation of a set of metacentrics, which became homozygous, which is not characteristic for parental forms, constituted an interesting model of speciation. The mechanisms of chromosome set selection should undoubtedly be determined in meiosis. The processes given the greatest importance were synapsis disorders, violated recombination, and a failure to pass the prophase of meiosis [36,37].

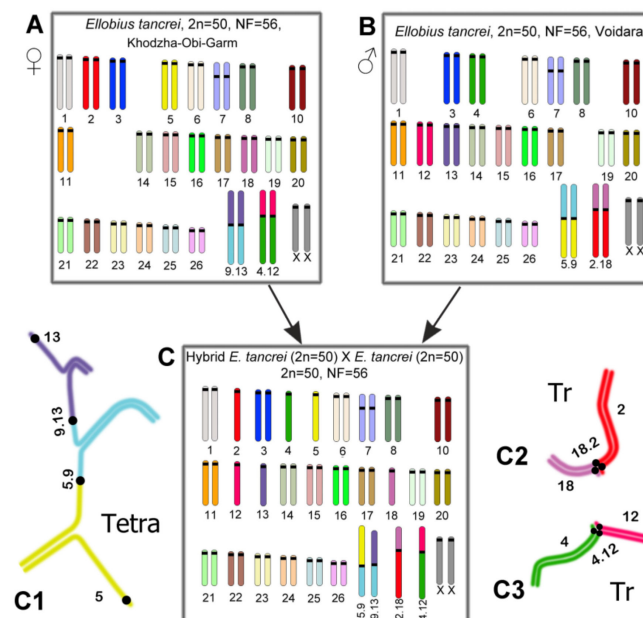


Figure 1. Scheme of experimental hybridization in *E. tancrei*. (A). “Khodzha Obi-Garm” form (female); $2n = 50$, $NF = 56$, 2Rb4.12 and 2Rb(9.13). (B). “Voidara” form (male); $2n = 50$, $NF = 56$, 2Rb2.18 and 2Rb5.9. (C). F1 hybrid with $2n = 50$, $NF = 56$, 1Rb2.18, 1Rb4.12, 1Rb5.9, and 1Rb(9.13). (C1). Scheme of SC tetraivalent (A5/Rb5.9/Rb9.13/A13). (C2,C3). Scheme of SC trivalents (A2/Rb2.18/A18) and (A4/Rb4.12/A12). The SC tetraivalent consisted of two Rb metacentrics with monobrachial homology and two acrocentrics (A5/Rb5.9/Rb9.13/A13).

In this work, we aimed to clarify the mechanisms for the rising reproductive barriers in mole vole hybrids carrying Robertsonian translocations, focusing on chromosome synapsis and recombination disorders during the meiotic prophase I.

2. Materials and Methods

2.1. Animals and Experimental Crossing

F10 (2n = 50, #27456; 2n = 49, #27430) *Ellobius tancrei* male hybrids were obtained as a result of the long-term experimental crossing of parental founders, differing in four pairs of Rb metacentrics and six pairs of acrocentrics [29,35]. All animals of the breeding lineage were karyotyped using routine and G-band techniques [38,39], and chromosome suspensions were deposited to the Large-Scale Research Facility “Collection of wildlife tissues for genetic research” IDB RAS, state registration number 3579666 and state contract 0088-2021-0019. Analysis of the results for F10 hybrids was carried out in comparison with the results of F1 hybrids (2n = 50, #26990, 26886, 26887) and homozygous males of *E. tancrei* (2n = 54, data from [28]).

2.2. Ethics

All applicable international, national, and institutional guidelines for the care and use of animals were followed. All experiments were approved by the Ethics Committee of the Vavilov Institute of General Genetics of the Russian Academy of Sciences, Russia (order No. 3 of 10 November 2016), and the Ethics Committee for Animal Research of the Koltzov Institute of Developmental Biology of the Russian Academy of Sciences, Russia (most recent order No. 37 of 25 June 2020). This article does not contain any studies with human participants performed by any of the authors.

2.3. Spreading Procedure

Spread meiotic chromosomes were obtained according to the method outlined in [40] with some modifications [32]. The testis was isolated, and then the tunic, fat, and large vessels were cut and removed. The testicular tubules were placed in Eagle’s medium without glutamine, minced using a fine razor blade, and homogenized with an automatic pipette. The cell suspension was transferred to a centrifuge tube, and the volume of the suspension was adjusted to 10 mL. After centrifugation of the suspension at 1500 rpm, the supernatant was discarded, the precipitate was diluted with eagle’s medium to a volume of 3 mL, and the suspension was homogenized. Six drops of a hypotonic solution (0.2 M) of sucrose were applied to the surface of a Teflon plate. One drop of cell suspension was applied to each drop of sucrose for 2 min. During this time, the nuclei of spermatocytes burst and expanded. Then, the surfaces of all drops were touched with the surface of a glass slide coated with poly-lysine. Thus, the spreading nuclei appeared on the surface of the glass slide. Then, the slides were transferred to the surface of a cooled plate and dried under a cold fan. Next, the preparations were fixed with a chilled 4% solution of paraformaldehyde (pH 9.2) containing 0.1 M sucrose. The preparations were washed in a 0.4% Photoflo solution and dried in air. After that, the slides were ready for immunostaining.

2.4. Primary and Secondary Antibodies

Primary antibodies. The following primary antibodies were used in this work: (1) mouse antibodies to the synaptonemal complex protein 3 (SCP3 or SYCP3) (ab97672, Abcam, Cambridge, UK) or rabbit to the SCP3 (ab15903, Abcam, Cambridge, UK) (both diluted to 1:100 or 1:250); (2) human polyclonal antibodies (CREST) against kinetochore proteins were used to localize centromeres (Fitzgerald Industries International, USA) diluted to 1:250; (3) mouse antibodies to the protein of mismatch reparations MLH1 for localization mature recombination nodules, (ab14206, Abcam, Cambridge, UK) (1:50); (4) antibodies to phosphorylated histone H2AX, also known as γ H2AFX, (ab26350, Abcam, Cambridge, UK) (1:500–1:1000), to identify areas of chromatin silencing.

Secondary antibodies. The following secondary antibodies were used in this work: goat anti-rabbit IgG conjugated with Alexa Fluor 488, goat anti-human IgG conjugated with Alexa Fluor 546, goat anti-mouse IgG conjugated with Alexa Fluor 546 or Alexa Fluor 555, chicken anti-rabbit IgG conjugated with Alexa Fluor 594, and goat anti-chicken IgG conjugated with Alexa Fluor 488 (all diluted to 1:300–800, Invitrogen, Carlsbad, CA, USA).

Antibodies were diluted in antibody dilution buffer (ADB) containing 3% bovine serum albumin (BSA) and 0.05% Triton X-100 in phosphate-buffered saline (PBS).

2.5. Immunostaining Procedure

Immunocytochemical study of the spread meiotic chromosomes was performed according to a previously described method [32,33]. Slides were washed with PBS and incubated with primary antibodies overnight at 4 °C. Slides were washed in PBS and incubated with secondary antibodies within 3 or 4 h at 37 °C in a humid chamber in a thermostatically controlled environment or at room temperature. Slides were washed in phosphate-buffered saline (PBS) and immersed into Vectashield with 4',6-diamidino-2-phenylindole (DAPI) (Vector Laboratories, Burlingame, CA, USA). Slides were analyzed using a Axio Imager D1 fluorescence light microscope (Carl Zeiss, Jena, Germany), the Genetic Polymorphisms Core Facility of the VIGG RAS (State Contracts, No 0092-2022-0002).

2.6. Statistical Analysis

The statistical analysis of all data was performed using GraphPad Prism 9 software (San Diego, CA, USA). Mean values (M) and standard deviation (SD) were calculated by the descriptive option of the software. The *p*-values reported in Table S1 were calculated by the Mann–Whitney two-sided non-parametric test. All diagrams were created by the graph options of the software.

3. Results

3.1. Hybrid Karyotype Diversity

We repeated the immunocytochemical study of the spread meiotic chromosomes in the F1 hybrids to obtain statistically significant results. All the F1 hybrids had the same karyotype, as we noted earlier [29] (Figure 1C), so the diversity of the karyotypes was observed from F2 onwards [35]. As follows from the schemes (Figure 1), the number of chromosomes ($2n = 50$) and the number of arms ($NF = 56$) coincided in the F1 hybrids and in both parents. However, the karyotypes of the F1 hybrids contained four unpaired Rb metacentrics each, Rb2.18, Rb4.12, Rb9.13, and Rb5.9 (Figure 1C), and six acrocentric univalents, A2, A4, A5, A12, A13, and A18 (Figure 1C).

As was demonstrated previously, there were 19 SC (synaptonemal complex) bivalents, including 19 autosomal bivalents formed by acrocentrics, and a bivalent of submetacentrics #7 (which is characteristic for *E. tancrei*) (Figure 2). The male sex (XX) chromosomes formed a sex bivalent with an extended asynapsis area. Ten chromosomes participated in the SC multivalents. The Rb2.18 and Rb4.12 metacentrics formed two SC trivalents with homologous acrocentrics, A2, A18 and A4, A12, respectively (Figure 1C3). The Rb9.13 and Rb5.9 metacentrics, which were homologous only by the arm corresponding to chromosome #9, formed the SC tetravalent A5/Rb5.9/Rb9.13/A13, including two acrocentrics, A5 and A13 (Figure 1C1). It should be emphasized that the SC tetravalent remained open in all the examined nuclei and was sometimes associated with other SCs (Table S1).

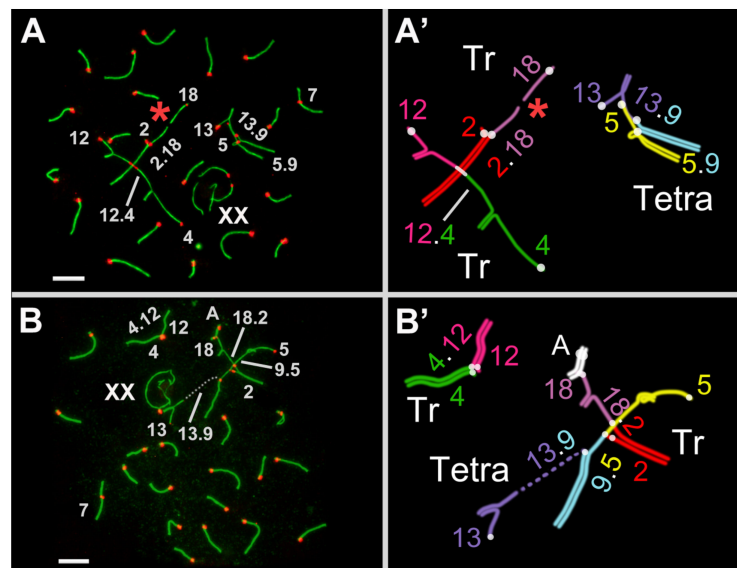


Figure 2. Prophase I spermatocytes of *E. tancrei* F1 hybrid. All spermatocytes in the image are at the early–mid pachytene transition stage. Immunostaining (A,B): axial and lateral elements of the SCs were identified using anti-SYCP3 antibodies (green); centromeres were identified using CREST antibodies to kinetochore protein (red). Schemes of the multivalents (A',B'). A—autosomal bivalent. Tr—trivalent. Tetra—tetraivalent. A red asterisk indicates univalent that has not yet entered synapsis. The numbers correspond to the numbers of chromosomes in Figure 1. Scale bar = 5 μm.

3.2. Features of Karyotypes of F9 and F10 Hybrids of *E. tancrei*

In the present experiment, we used the descendants of the F1 sibs, up to F9 and F10, that were obtained in strictly inbred crosses (Figure 3). Their karyotypes varied due to either the homo- or heterozygous state of the Rbs.

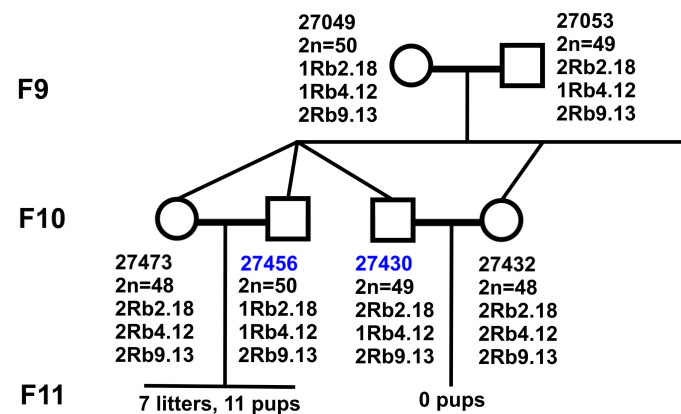


Figure 3. Crossing scheme for F9 hybrids. Peculiarities of karyotypes of F9 hybrids and their descendants in F10. Diploid numbers, Rb metacentrics, and relatedness of F9 (parental form) and F10, studied in fertile male #27456 and sterile male #27430.

The main results were obtained for the F10 hybrids; one of them, a fertile male (#27456, 2n = 50, 1Rb2.18, 1Rb4.12, and 2Rb9.13), inherited the karyotype of the father, while the other, a sterile male (#27430, 2n = 49, 2Rb2.18, 1Rb4.12, and 2Rb9.13) inherited the karyotype of the mother (Figure 3). Their partners, F10 female sibs, had an identical completely homozygous karyotype (2n = 48, 2Rb2.18, 2Rb4.12, and 2Rb9.13), which allowed us to exclude their contribution to the fertility disorders.

In all of the sixteen crosses of the F1 hybrids, the offspring were obtained, while two out of the eleven pairs of F10 hybrids had no offspring. In one of these pairs, the female had two uterine scars, indicating embryo resorption, which suggests the fertility of a male.

Another non-virgin female #27432 (in a cross with the F10 male #27430) had no uterine scars, which persist for a long time in a mole vole's uterus and mark embryos or resorption in the absence of born cubs. Thus, the sterility of the F10 male (#27430) appeared to be complete, which was an exceptional case in our long-term breeding practice of this line. In all the cases of infertile pairs, except for this one, uterine scars were found in the females.

The fertile F9 female #27481 and male #27455 had karyotypes identical to the fertile F10 male #27456, $2n = 50$, $1Rb2.18$, $1Rb4.12$, and $2Rb9.13$ (Figure 3).

3.3. Immunocytochemical Study of Spread Nuclei of Primary Spermatocytes of Sterile and Fertile F10 Hybrids

The results of the immunocytochemical analysis of the spermatocyte nuclei of the F10 hybrids at the mid and late pachytene stages were fully consistent with the results of a prognostic analysis of their karyotypes (Figure 3). However, the pathway to the completion of synapsis, at the late zygotene and pachytene stages, was a complicated and protracted one.

Leptotene. Thin, discontinuous axial elements of chromosomes, which progressively lengthened, were revealed in the nuclei of the spermatocytes at the leptotene stage (Figure 4).

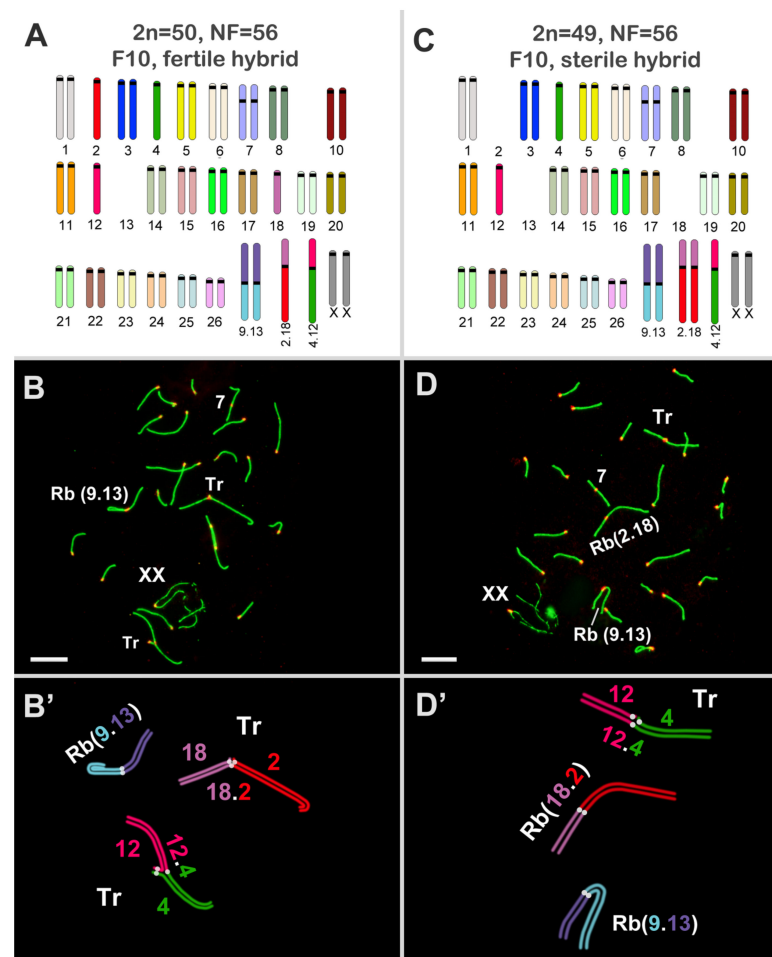


Figure 4. Karyotype schemes and chromosome synapsis during meiotic prophase I in spermatocytes of experimental fertile hybrid #27456 (A,B,B') and sterile hybrid #27430 (C,D,D') of *E. tancrei*. (A). Chromosomes of fertile F10 hybrid: $2n = 50$, $NF = 56$, $1Rb2.18$, $1Rb4.12$, and $2Rb(9.13)$. (B). Pachytene spermatocytes of fertile F10 hybrid: two SC trivalents, $Tr(2/2.18/18)$ and $(4/4.12/12)$ (see schemes in B'). (C). Chromosomes of sterile F10 hybrid: $2n = 49$, $NF = 56$, $2Rb2.18$, $1Rb4.12$, and $2Rb(9.13)$. (D). Pachytene spermatocyte of sterile F10 hybrid: one SC trivalent, $Tr(4/4.12/12)$ (see schemes in D'). Axial and lateral elements of the SCs were identified using anti-SYCP3 antibodies (green); centromeres were identified using "CREST" antibodies to kinetochore protein (red). Scale bar (B,D) = 5 μ m.

Zygotene. At the zygotene stage, the axial elements of chromosomes were completed, and then their adjustment and the synapsis of homologues took place. The thin, highly stretched axial elements of chromosomes began to synapse from telomeric ends, and short sections of SCs developed between them. Small SC bivalents were the first to complete synapsis.

Partially synapsed chromosomes formed complex chains of open SC trivalents and occasionally involved SC bivalents (Figure 5E). The peculiarities of axial element formation, the onset of axial element synapsis, and chromatin silencing at the leptotene and mid zygotene stages were similar in the fertile and sterile hybrids.

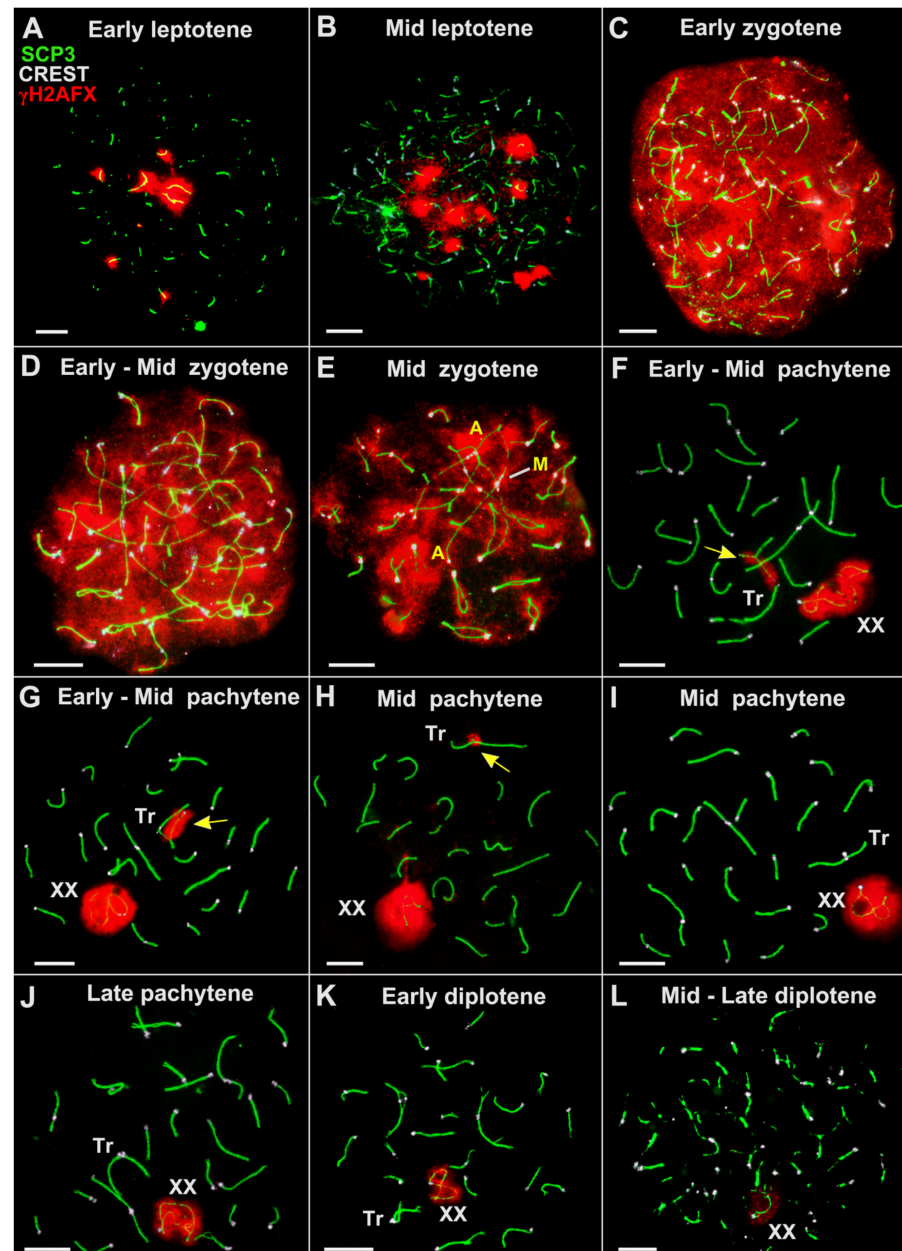


Figure 5. Dynamics of chromosome synapsis and chromatin silencing in spermatocytes of *E. tancrei* sterile F10 hybrid during prophase I (A–L). Axial and lateral elements of the SCs were identified using anti-SYCP3 antibodies (green); centromeres were identified using “CREST” antibodies to kinetochore proteins (white) (except for (A,H)); and chromatin inactivation was revealed using anti- γ H2AFX antibodies (red). XX—male sex bivalent. Tr—SC trivalent. (A)—autosomal bivalent. The yellow arrow indicates the γ H2AFX-positive asynaptic regions of SC trivalent (F–H). A similar set of microphotographs (without γ H2AFX) are shown in Figure S1. Scale bar (A–L) = 5 μ m.

We were unable to detect spermatocytes at the bouquet stage in any of the studied hybrids (F1 and F10).

Pachytene. Synapsis of most of the paired autosomes was completed by the pachytene stage. In accordance with the “synapsis or silencing” formula [41], after synapsis and DSBs DNA repair, the silencing of the chromatin of paired autosomes was gradually completed.

In the sterile F10 hybrid #27430, two SC bivalents, 2Rb9.13 and 2Rb2.18, were clearly detected in the spread spermatocytes at the early and mid pachytene stages (Figure 5F,J). A considerable delay in the formation of SC trivalent and SC bivalents of Rbs can be regarded as a significant disorder. Approximation of the centromeric ends of two nonhomologous acrocentrics (that are part of the SC trivalent) was chaotic in both the fertile and sterile F10 males. Multiple temporal associations of telomeres of nonhomologous chromosomes were observed (Figures 5 and 6). The open SC trivalents entered into associations with each other, and short SCs were formed between the pericentromeric sites of nonhomologous acrocentrics (Figure 6B).

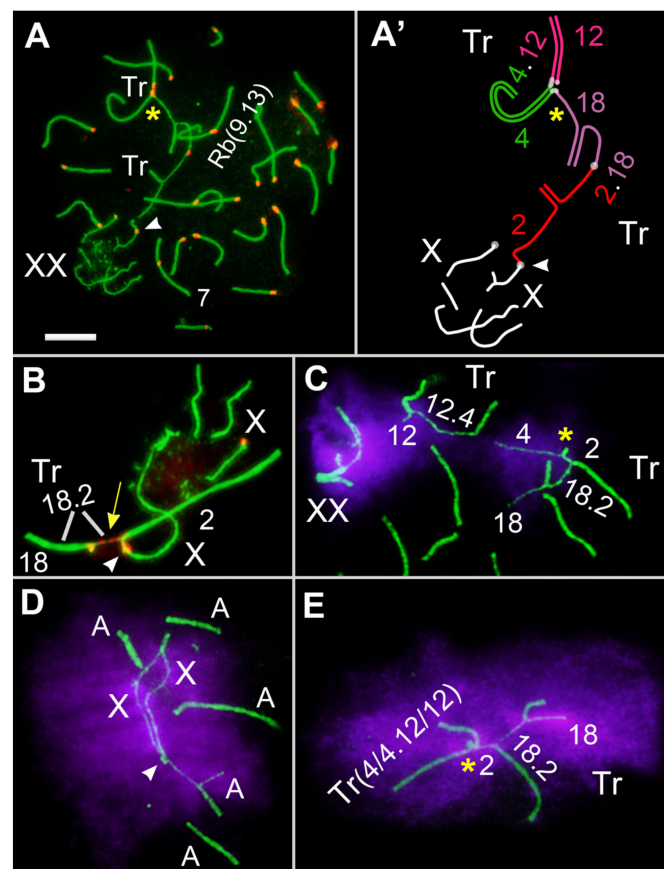


Figure 6. Chromosomes associations in spermatocytes of *E. tancrei* fertile F10 hybrid #27456 (A–E), early–mid pachytene stage. Axial and lateral elements of the SCs were identified using anti-SYCP3 antibodies (green); centromeres were identified using “CREST” antibodies to kinetochore proteins (red); and chromatin inactivation was revealed using anti- γ H2AFX antibodies (magenta). Two trivalents, (Tr(A2/Rb2.18/A18) and Tr(A4/Rb4.12/12)), were formed in the hybrid. (A)—autosomal bivalent. Tr—trivalent. The white arrowhead indicates nonhomologous synapsis of short arms of XX and autosomes or acrocentrics of SC trivalent. The yellow asterisk indicates nonhomologous synapsis of short arms of acrocentrics of two trivalents (SCs chain; (A,A',C,E)). The yellow arrow indicates the stretched centromere of the metacentric in the SC trivalent (B). The numbers correspond to the numbers of chromosomes in Figure 4A. Scale bar (A) = 5 μ m.

The chromatin of the asynaptic chromosome sites remained inactivated and bound to histone γ H2AFX (Figure 5). It is worth highlighting that the synapsis of three chromosomes forming the SC trivalent in the fertile male #27456 was prolonged (Figure 6).

Gaps were often revealed in the structure of the asynapsed and stretched sections of the axial elements in the slow SC trivalents, which also delayed the complete arrangement of the SC trivalents. The presence of gaps in the pericentromeric regions of the axial elements of the Rb metacentrics and acrocentrics, which are part of the SC trivalents, is a transient phenomenon [23]. We considered these events to be a synaptic adjustment.

A delay in chromosome synapsis at early pachytene stages was more often observed in two SC trivalents and less often in the SC bivalents (Table S1). At the early pachytene stage, an open SC trivalent, A4/Rb4.12/A12, was found in 9.96% of the nuclei in the fertile F10 male #27456 and in 17.85% of the nuclei in the sterile F10 male #27430; the differences were not significant, while in the F1 hybrids, this index was significantly higher at 76.13% (Figure 7, Table S1). It is probable that these significant differences can be explained by the delayed synaptic adjustment due to the presence of more complex figures, a tetravalent, in particular. A similar set of microphotos (without γ H2AFX) are shown in Figure S1.

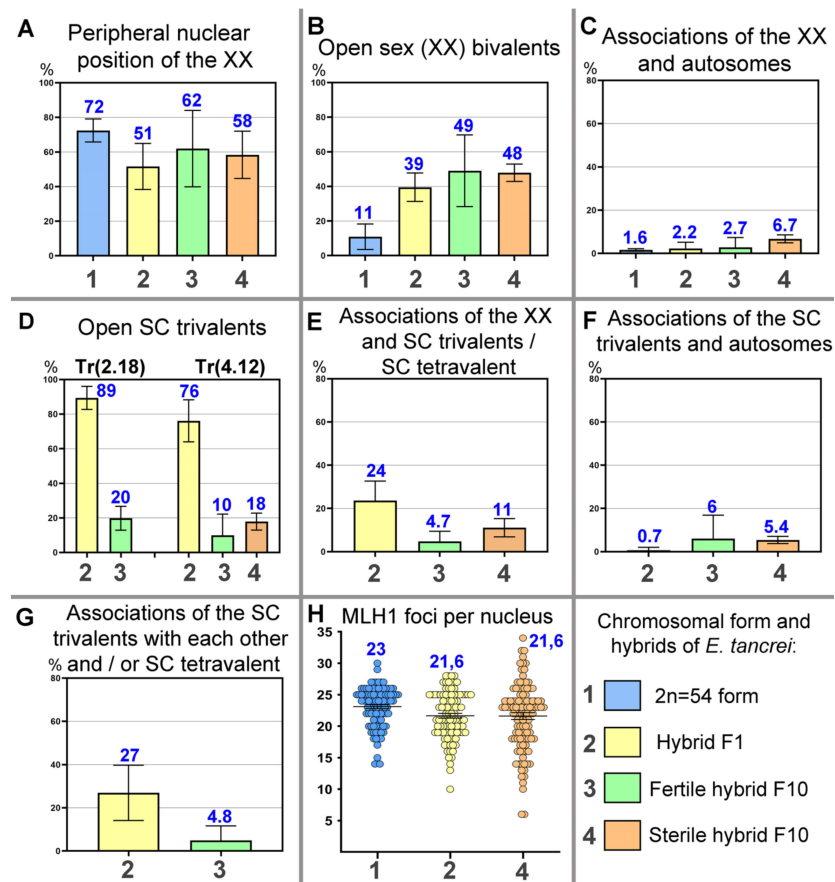


Figure 7. Diagram representation of different meiotic parameters in spermatocytes of the chromosomal form and hybrids of *E. tancrei*. All data are taken from Table S1. The colors of the columns in the diagram correspond to mole voles: blue for $2n = 54$ form, yellow for F1 hybrid, light green for a fertile F10 hybrid, and pale orange for a sterile F10 hybrid. The blue numbers represent the percentage for each column (A–G) or the average number of MLH1 signals (H). The black numbers in the diagrams correspond to form and hybrids (see captions under diagram F). (A) Number of nuclei (%) with peripheral nuclear position of sex (XX) bivalent. (B) Number of nuclei (%) with open configuration of sex (XX) bivalent. (C) Number of nuclei (%) with associations with XX bivalent and autosomes. (D) Number of nuclei (%) with open configurations of SC trivalents (left—SC trivalent Tr2.18; right—Tr4.12). (E) Number of nuclei (%) with associations with XX bivalent and SC trivalents/SC tetravalent. (F) Number of nuclei (%) with associations with SC trivalents and autosomes. (G) Number of nuclei (%) with associations with SC trivalents with each other and/or SC tetravalent. (H) Dot plot of the average number of MLH1 foci per nucleus.

Diplotene. At the *diplotene* stage, a gradual degradation of the desynaptic axial elements of the chromosomes occurred (Figure 5K,L).

3.4. Sex XX Bivalent: Formation and Associations with Autosomes

In both F10 hybrids, it was difficult to identify the XX bivalent during the early stages of the prophase. Firstly, this was due to the chromosome chains' complexity and, secondly, because histone γ H2AFX was associated with all the asynapsed regions of the chromosomes, appearing to be a manifestation of the meiotic silencing of the unsynapsed chromatin (MSUC) and meiotic sex chromosome inactivation (MSCI). However, the XX bivalent was clearly detected in the nuclei in which the synapsis of paired autosomes was complete, and the histone γ H2AFX only persisted in the open SC trivalents and the sex chromosomes (Figures 5, 6 and 8).

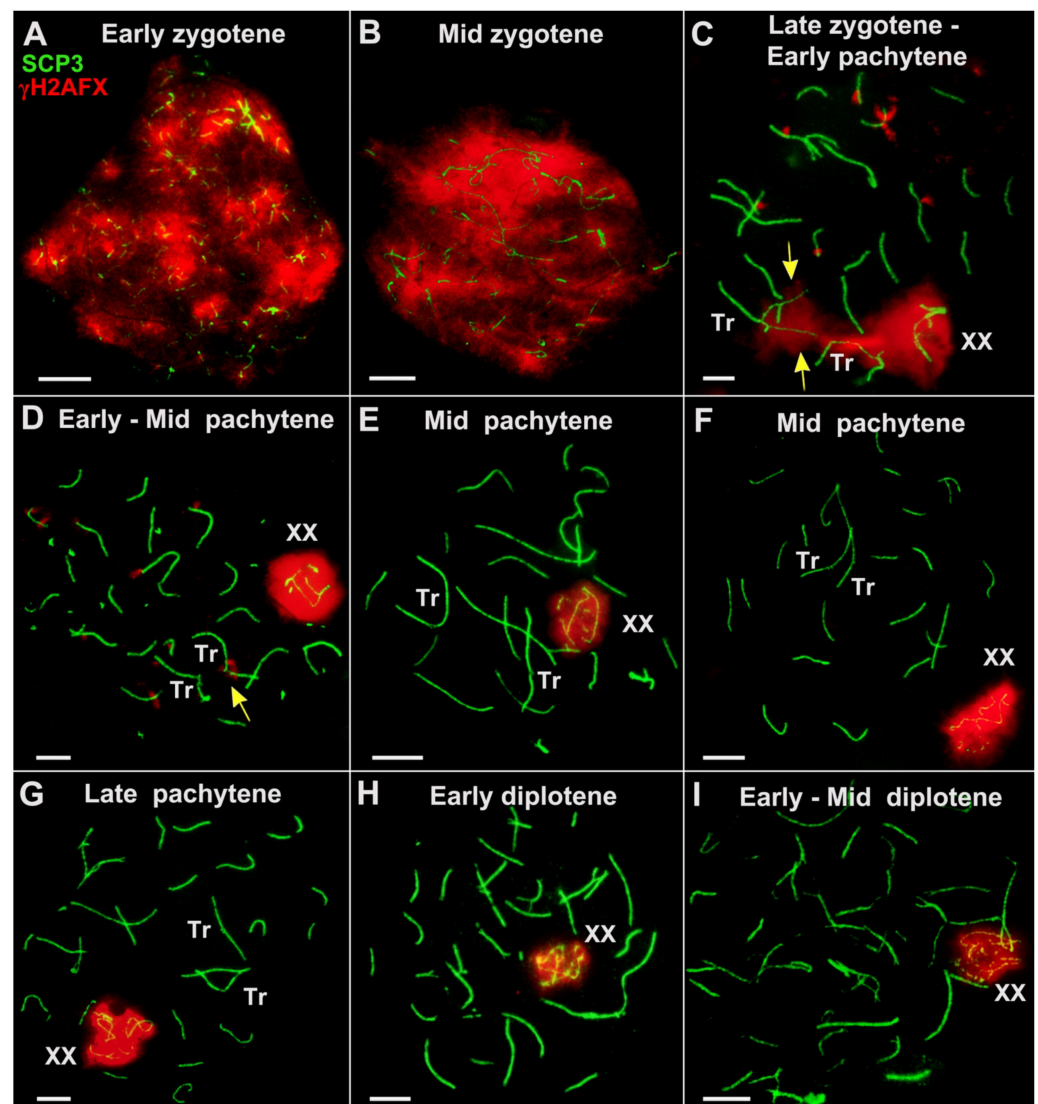


Figure 8. Dynamics of chromosome synapsis, chromatin silencing, and reactivation in spermatocytes of the *E. tancrei* fertile F10 hybrid during prophase I (A–I). Axial and lateral elements of the SCs were identified using an anti-SYCP3 antibody (green); and chromatin inactivation was revealed using an anti- γ H2AFX antibody (red). XX—male sex bivalent. Tr—SC trivalent. The yellow arrow indicates the γ H2AFX positive asynaptic regions of SC trivalent (C and D). Scale bar (A–I) = 5 μ m.

The XX bivalent was regularly associated with both the open SC trivalents and the chains of two SC trivalents, and it was sometimes placed nearby them (Figure 4).

Open XX bivalents were detected in almost 49% of the pachytene nuclei of the F10 males (Figure 6, Table S1), whereas in the homozygous form of *E. tancrei*, $2n = 54$, open XX bivalents were found much less frequently, i.e., in 11% of the nuclei.

None of the analyzed parameters (Figure 7) significantly differentiated the sterile F10 male #27430 from the fertile F1 and F10 males except for the single parameter “multivalent associations”. The latter was due to the fact that not fully synapsed acrocentrics in open tetravalents more often enter into associations in the spermatocytes of F1 hybrids. The sterile male #27430 had significant differences from the standard *E. tancrei* $2n = 54$ male, which was related to the number of nuclei with associations with the XX bivalent and autosomes, i.e., $M \pm SD$ and the percentage of nuclei, which reached 6.74% versus 1.65%.

The associations of trivalents with the XX bivalent deserve more attentive consideration. In the fertile F10 hybrid #27456, this index was significantly lower than in the F1 hybrids (Figure 6, Table S1); all these hybrids formed two trivalents. In the sterile F10 hybrid #27430, associations with a sex bivalent and a single trivalent were observed more frequently; 11.09% for a single trivalent versus 4.73% for two trivalents in the fertile F10 male #27456 (Figure 7, Table S1). Although the differences were not significant, two trivalents were formed in the fertile hybrid instead of one in the sterile hybrid. Thus, it turns out that such associations were observed almost four times more often than in the fertile F1 and F10 hybrids. It is probable that this was the main disorder that led to the sterility of this male.

After the completion of SC trivalent formation, at the mid–late pachytene stages, the histone γ H2AFX in most of the nuclei was exclusively detected in association with the chromatin of the sex chromosomes (Figure 8E–I). Then, the sex bivalent gradually moved to the periphery of the nucleus. Thus, the typical structure of the sex body in all the studied types of hybrids was formed, which corresponded to the norm, $2n = 54$.

3.5. Patterns of Recombination in F10 Hybrids

The distribution of late recombination nodules in the SC structure in F10 hybrids was examined using the antibodies of the mismatch repair protein MLH1 (Figure 9). MLH1 protein foci were formed early in the SC structure of the trivalents between the acrocentrics and the Rb metacentric. The MLH1 protein foci were always localized in the distal parts of the SC trivalents. On the one hand, this ensured the strong connection of these three chromosomes throughout the entire prophase I of meiosis and the correct segregation of the chromosomes at the M1 stage. On the other hand, the long asynaptic ends of the acrocentrics could be in nonhomologous contact with the autosomes.

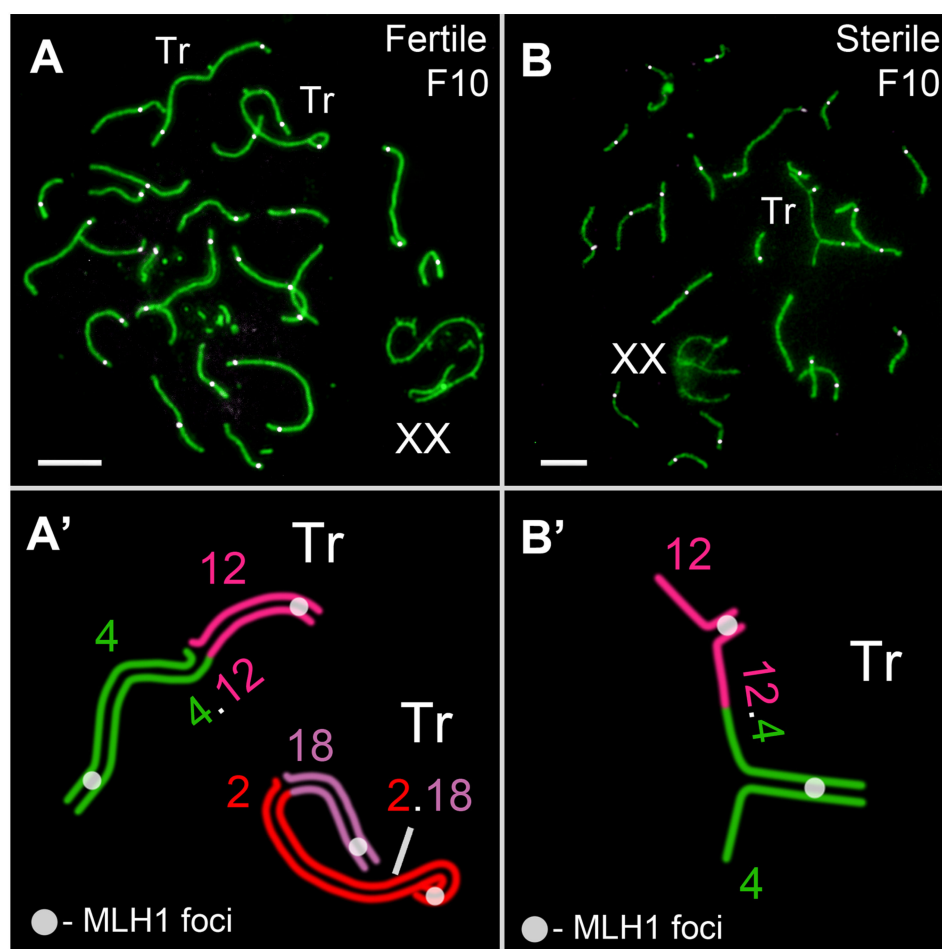


Figure 9. Recombination in *Ellobius tancrei* F10 hybrids. Axial elements were identified using anti-SYCP3 antibodies (green). Anti-MLH1 antibodies (white) were used as a marker of recombination nodules. (A). Pachytene spermatocyte of fertile F10 hybrid. Two closed SC trivalents, Tr(2/2.18/18) and Tr(4/4.12/12), with one MLH1 signal per arm (see schemes in (A')). (B) Pachytene spermatocyte of sterile F10 hybrid. Open SC trivalent Tr(4/4.12/12) with one MLH1 signal per arm (see schemes in (B')). Scale bar = 5 μ m.

The number of MLH1 signals in the fertile male was slightly higher than, but significantly different to the F1 hybrid and the sterile F10 hybrid (Figure 7, Table S1). This may be due to the absence of MLH1 signals in some bivalents in the hybrid spermatocytes. However, no differences between the hybrids themselves were found in this indicator (Figure 7, Table S1).

Therefore, despite the numerous challenges, the complex configurations of the chromosomes during prophase I did not necessarily imply cell elimination and complete failure of gametogenesis.

4. Discussion

The process of spermatogenesis consists of three main stages [42–44]:

Stage I—Spermatocytogenesis, a stage during which the spermatogonia divide mitotically and some of them turn into primary spermatocytes;

Stage II—Spermatidogenesis, a long stage during which the primary spermatocytes undergo the complex prophase I of meiosis, and the first (reductive) division forms secondary spermatocytes, which in turn overcome the second division of meiosis, resulting in the formation of round haploid spermatids;

Stage III—Spermiogenesis, a stage during which round spermatids differentiate into elongated spermatids and then differentiate into mature motile spermatozoa that are ready for fertilization as they move through the ducts of the epididymis.

Genetic control of the process occurs at all stages of spermatogenesis. In meiosis, the most-studied checkpoints at which the selection of spermatocyte development proceeds include strict checkpoints controlling the pachytene stage, the longest stage of prophase I of meiosis, and the spindle assembly checkpoint in the metaphase [3,45,46].

Our results demonstrated that the reduced fertility in the hybrids with Robertsonian translocations was caused mainly by the cumulative effect of different disorders rather than by the number and complexity of the figures formed in the prophase I of meiosis, as was previously described for mole voles, lemurs, and mice [9,20,23,24,30,47]. The decrease in fertility, up to sterility, in the mole vole hybrids with one or two trivalents was affected by the following: (1) the violation of the entire architectonics of the spermatocyte nuclei at the early zygotene–early pachytene stages; (2) the slowed rate of synapsis of the trivalents and Rb bivalents in the transition from the zygotene stage to the pachytene stage; (3) the associations of autosomal bivalents and trivalents with the XX sex chromosomes; (4) the altered configuration of the sex bivalent; and (5) the features of inactivation (MSCI). In addition, impaired spermatogenesis can be due to genetic or epigenetic instability, leading to the dysregulation of gene expression and the occurrence and inheritance of random mutations.

Within our experiment, the prospective impact of homozygous Robertsonian chromosomes should also be taken into account. Evidently, Rbs alter the nuclear architecture of meiotic prophase spermatocytes [26]. Such changes overlap with global restructuring: meiotic prophase nuclei lose topologically associating domains, which occur in interphase [37]. Nevertheless, chromosomes maintain their chromosome territories. When big Rbs are formed from the large acrocentrics that occupy spatially distant territories in the nucleus, significant disturbances probably occur, which we described as synapsis retardation. It is important to note that in this case we are referring to bivalents.

The most intricate picture of synapsis was shown by the six unpaired chromosomes, which formed two SC trivalents in the prophase I of meiosis in the fertile F10 hybrid #27456, and by the three unpaired chromosomes that formed a single SC trivalent during meiosis in the sterile F10 hybrid #27430. If the Rb metacentric, for example, Rb4.12, was inherited by the hybrid from a male of the parental form, then two homologous acrocentrics, A4 and A12, were inherited by it through a series of generations from a female of another parental form. Since we are talking about founders from isolated populations, we cannot exclude the formation of differences in the structure of the pericentromeric sites of the three chromosomes that formed the SC trivalent. The possibility that these differences were formed due to DNA satellites, as the most variable part of the genome that is involved in formation of chromocenters, in association with autosomes and sex chromosomes and in association with the sex bivalent with autosomes, seems most probable.

However, an even more evident reason for the delayed synapsis of chromosomes within SC trivalents seems to be the violation of the meiotic nuclei architecture.

We previously classified Rb SC trivalents as either fast or slow when studying intraspecific hybrids of mole voles that were heterozygous for 10 Rb metacentrics [23]. The fast trivalents had completed synapsis by the onset of the pachytene stage. They included short Rb metacentrics and, correspondingly, short acrocentrics, but, most importantly, the distal ends of the chromosomes lay close to each other, which did not lead to stretching of these trivalents or the homozygous Rb metacentrics between their attachment points to the nuclear envelope. Here, we demonstrated that in the sterile hybrid F10 #27430, both large bivalents, 2Rb9.13 and 2Rb2.18, showed delayed synapses.

The slow SC trivalents, which had a long length of the zone of their attachment to the nuclear envelope, were at a great distance from each other, which led to a strong stretching of the pericentromeric area of the metacentric. At the same time, the acrocentrics, which were also attached to the nuclear envelope, could not move quickly to the pericentromeric region of the Rb metacentric. The distinct input of different Rbs to meiosis impairment

was demonstrated in mice [48,49]; for example, heterozygotes by Rb(16.17)8Lub and Rb(9.19)163H demonstrated a diverse frequency of nondisjunction [50].

The relationships between the open SC trivalents and the sex XX bivalent deserve special attention because the associations with sex bivalents in male meiosis are the very ones that terminate the cell. In the case of *E. tancrei*, the sex bivalent of males is represented by isomorphic XX chromosomes. Both X chromosomes are identical in the G-band picture [31], but in male meiosis, they clearly demonstrate typical male behavior; they synapse only partially, the chromatin undergoes silencing, and, starting from the mid pachytene stage, the XX bivalents are dislocated to the nucleus periphery and form the sex body [33,51]. The most fascinating cases in the hybrids were chaotic associations of the XX chromosomes with autosomes. For example, one X chromosome was associated with acrocentric A4, and the second X chromosome was associated with acrocentric A12, which is part of the same open SC trivalent, Tr A4/Rb 4.12/12 (Figure 5). Before the synapsis of the SC trivalents was completed, the sex chromosomes of these hybrids had a configuration and structure that differentiated them from the homozygous forms of *E. tancrei* [33]. The multiple associations of open, incompletely synapsed SC trivalents with sex XX bivalents, which we observed in the F10 hybrids, manifest a triggering mechanism for pachytene arrest, which ends in apoptosis and, thus, the selection of defective spermatocytes. The most important signs of pachytene arrest are also chromatin silencing in the asynaptic regions of autosomes and the partial reactivation of the chromatin of sex chromosomes [52–54]. In the hybrids we described, we did observe the mentioned signs at the late zygotene or early pachytene stages for numerous cells. In the cells avoiding such an impaired meiotic development synapsis correction, which occurred in the mid–late pachytene, a typical sex body was formed in the spermatocyte nuclei, with a chromatin that was intensively immunostained with antibodies to histone γ H2AFX. Minor traces of γ H2AFX were occasionally seen only in the single SC trivalents (Figures 5H and 8D).

The aforementioned dynamics of chromatin synapsis activity correspond to the data of [55], in which mice that were heterozygous for 8 Rb translocations were studied. In this case, the high frequency of the meiotic silencing of the non-synapsed chromatin did not lead to an interruption of meiosis at the pachytene stage. A portion of the spermatocytes in the males of these mice underwent apoptosis at the metaphase I stage.

We suggest that the results of another study [55,56] and our results regarding the bivalents' and trivalents' associations with XX sex chromosomes correlated with the existing data [57]. One of the most important results obtained in [57] is the proof of the transient alternating ectopic contacts of the XY sex bivalent (in the absolute majority of cases, it was the X chromosome), with each of the autosomal 19 SC bivalents existing in mouse spermatocyte nuclei. The organization of spermatocyte nuclear architectonics at the prophase I stage of meiosis, interchromosomal interactions, and the role of pericentromeric DNA satellites in these processes should be studied further in mole voles.

In most species of eukaryotes, the transition of spermatocytes from the leptotene stage to the zygotene stage appears to be associated with the formation of the bouquet stage. This is a crucial, genetically controlled stage of the prophase of meiosis [58,59]. First, as has been figuratively put, "the bouquet ties the ends together" [58]. The bouquet stage is followed by the alignment of the axial elements of the homologues and the beginning of their synapsis. In mice with two pairs of homologous Rb metacentrics, ref. [26] described an interesting feature of the bouquet formation organization: at the stage of the bouquet, the telomeres of the acrocentrics were grouped separately from the four telomeres of the Rb metacentrics. It should be emphasized that this stage follows the classical scenario in homozygous forms of *E. tancrei* [33]. However, while studying this experimental line of *E. tancrei*, we were never able to detect spermatocytes at the bouquet stage in the hybrids heterozygous for Rb translocations. Obviously, we cannot completely exclude the possibility that this stage is passed quickly and that we simply did not detect it in the preparations of the spread nuclei. Further difficulties in terms of synapsis and the peculiarities of related MSUC processes

may also be caused by the non-standard transition of meiosis from the leptotene stage to the zygotene stage.

No analogous experiment has been carried out on mice throughout a number of generations, though several experiments reaching the third generation and backcrosses, as well as a diverse analysis of the genetic features of natural hybrid zones, have drawn the same conclusions [30,60]; Rbs can reduce gene flow due to hybrid failure. In contrast to the data obtained in mice [27,55], the disturbances in mole voles turn out to be more complex. Inconsistency with the norm indicates significant abnormalities in the spatial arrangement of chromosomes, which changes the dynamics of the meiosis patterns. They start with the absence of the chromosome bouquet in the zygotene stage, the delayed synapsis of the bivalents and trivalent in the pachytene stage, and the alteration of the recombination and irregular contacts of the autosomes with the sex bivalent at the early prophase I stage.

The postzygotic reproductive barriers considered in this paper, which ensured the complete and partial sterility of the hybrids, were in good agreement with the ideas about the mechanisms of speciation outlined in the BSC (Biological Species Concept, [61,62]) and later in the HHS concept (Homoploid Hybrid Speciation, [63,64]). The BSC emphasizes the importance of forming a protected gene pool without focusing on rigid reproductive barriers, whereas the HHS concept implies the process of the emergence of a new, reproductively isolated species through hybridization and the combination of parts of the parental genomes without increasing ploidy. For organisms with Robertsonian chromosomal variability, the formation of postzygotic reproductive isolation in hybrid offspring by sorting chromosomes and gene alleles leads to genomic or gene incompatibility between the nascent hybrid and both parent species, which can be considered as one of the intrinsic postzygotic barriers in speciation [65–67]. A comprehensive analysis of natural house mouse populations suggests that Rbs can accelerate the speciation process through racing zonation, especially in islands [68]. The restricted introgression between rock-wallabies with numerous Rbs demonstrated a further enhancement of divergence at the species level [69].

Whether reproductive isolation in hybrids or sympatric speciation does not have to be complete is actively debated [70–72]. A number of models support this thesis [73–77]. We believe the presented case of the experimental hybridization of the chromosomal forms of mole voles illustrates well the view that the decline in hybrid fertility can be determined by different causes. Gametogenesis disorders can be diverse, which makes a thorough stage-by-stage analysis of meiosis development necessary.

Overall, the changes in the nuclear architecture specific to the prophase I of meiosis can accentuate the alterations caused by the presence of Rbs, suggesting that various translocations have divergent effects on the degree of meiosis failure, spermatogenesis, and fertility.

Supplementary Materials: The following supporting information can be downloaded at: <https://www.mdpi.com/article/10.3390/d15030364/s1>, Figure S1: Chromosome dynamics in prophase I of *E. tancrei* sterile F10 hybrid. Table S1: Meiotic data of *E. tancrei* and hybrids.

Author Contributions: Conceptualization, O.K., S.M. and I.B.; methodology, O.K. and S.M.; investigation, O.K., S.M., V.T., M.P. and I.B.; writing, O.K., I.B., V.T. and S.M.; visualization, S.M.; funding acquisition, O.K. All authors have read and agreed to the published version of the manuscript.

Funding: This research was supported by the Russian Science Foundation, grant No. 22-24-01163.

Institutional Review Board Statement: Not applicable.

Data Availability Statement: Not applicable.

Acknowledgments: We thank the Genetic Polymorphisms Core Facility of the Vavilov Institute of General Genetics of the Russian Academy of Sciences for the use of microscopes.

Conflicts of Interest: The authors declare no conflict of interest.

References

1. Darwin, C. *On the Origin of Species by Natural Selection*; Murray: London, UK, 1859.
2. Morelli, M.A.; Cohen, P.E. Not all germ cells are created equal: Aspects of sexual dimorphism in mammalian meiosis. *Reproduction* **2005**, *130*, 761–781. [[CrossRef](#)] [[PubMed](#)]
3. Subramanian, V.V.; Hochwagen, A. The meiotic checkpoint network: Step-by-step through meiotic prophase. *Cold Spring Harb. Perspect. Biol.* **2014**, *6*, a016675. [[CrossRef](#)] [[PubMed](#)]
4. Ayala, F.J.; Coluzzi, M. Chromosome speciation: Humans, *Drosophila*, and mosquitoes. *Proc. Natl. Acad. Sci. USA* **2005**, *102* (Suppl. 1), 6535–6542. [[CrossRef](#)] [[PubMed](#)]
5. White, M.J.D. *Modes of Speciation*; Freeman: San Francisco, 1978.
6. King, M. *Species Evolution: The Role of Chromosome Change*; Cambridge University Press: Cambridge, UK, 1993.
7. Matveevsky, S.N.; Kolomiets, O.L. Karyotype variability: Chromosomal rearrangements, meiotic manifestation in mammals and evolutionary consequences. *Russ. Found. Basic Res. J.* **2020**, *106*, 50–59. [[CrossRef](#)]
8. Gropp, A.; Winking, H.; Zech, L.; Müller, H. Robertsonian chromosomal variation and identification of metacentric chromosomes in feral mice. *Chromosoma* **1972**, *39*, 265–288. [[CrossRef](#)]
9. Capanna, E.; Castiglia, R. Chromosomes and speciation in *Mus musculus domesticus*. *Cytogenet. Genome Res.* **2004**, *105*, 375–384. [[CrossRef](#)]
10. Searle, J.; Zima, J.; Polly, P. *Shrews, Chromosomes and Speciation*; Searle, J., Polly, P., Zima, J., Eds.; Cambridge University Press: Cambridge, UK, 2019; pp. 455–462. [[CrossRef](#)]
11. Nevo, E.; Ivanitskaya, E.; Beiles, A. *Adaptive Radiation of Blind Subterranean Mole Rats: Naming and Revisiting the Four Sibling Species of the *Spalax ehrenbergi* Superspecies in Israel: *Spalax galili* (2n = 52), *S. golani* (2n = 54), *S. carmeli* (2n = 58) and *S. judaei* (2n = 60)*; Backhuys Publishers: Leiden, The Netherlands, 2001.
12. Lyapunova, E.A.; Vorontsov, N.N.; Korobitsina, K.V.; Ivanitskaya, E.Y.; Borisov, Y.M.; Yakimenko, L.V.; Dovgal, V.Y. A Robertsonian fan in *Ellobius talpinus*. *Genetica* **1980**, *52–53*, 239–247. [[CrossRef](#)]
13. Lyapunova, E.A.; Bakloushinskaya, I.Y.; Saidov, A.S.; Saidov, K.K. Dynamics of chromosome variation in mole voles *Ellobius tancrei* (Mammalia, Rodentia) in Pamiro-Alay in the period from 1982 to 2008. *Russ. J. Genet.* **2010**, *46*, 566–571. [[CrossRef](#)]
14. Romanenko, S.A.; Lyapunova, E.A.; Saidov, A.S.; O'Brien, P.; Serdyukova, N.A.; Ferguson-Smith, M.A.; Graphodatsky, A.S.; Bakloushinskaya, I. Chromosome translocations as a driver of diversification in mole voles *Ellobius* (Rodentia, Mammalia). *Int. J. Mol. Sci.* **2019**, *20*, 4466. [[CrossRef](#)]
15. Bakloushinskaya, I.; Lyapunova, E.A.; Saidov, A.S.; Romanenko, S.A.; O'Brien, P.C.; Serdyukova, N.A.; Ferguson-Smith, M.A.; Matveevsky, S.; Bogdanov, A.S. Rapid chromosomal evolution in enigmatic mammal with XX in both sexes, the Alay mole vole *Ellobius alaicus* Vorontsov et al., 1969 (Mammalia, Rodentia). *Comp. Cytogenet.* **2019**, *13*, 147–177. [[CrossRef](#)]
16. Tambovtseva, V.; Bakloushinskaya, I.; Matveevsky, S.; Bogdanov, A. Geographic mosaic of extensive genetic variations in subterranean mole voles *Ellobius alaicus* as a consequence of habitat fragmentation and hybridization. *Life* **2022**, *12*, 728. [[CrossRef](#)]
17. Hattori, A.; Fukami, M. Established and novel mechanisms leading to de novo genomic rearrangements in the human germline. *Cytogenet. Genome Res.* **2020**, *160*, 167–176. [[CrossRef](#)]
18. Ur, S.N.; Corbett, K.D. Architecture and dynamics of meiotic chromosomes. *Annu. Rev. Genet.* **2021**, *55*, 497–526. [[CrossRef](#)]
19. Grize, S.A.; Wilwert, E.; Searle, J.B.; Lindholm, A.K. Measurements of hybrid fertility and a test of mate preference for two house mouse races with massive chromosomal divergence. *BMC Evol. Biol.* **2019**, *19*, 25. [[CrossRef](#)]
20. Moses, M.J.; Karatsis, P.A.; Hamilton, A.E. Synaptonemal complex analysis of heteromorphic trivalents in Lemur hybrids. *Chromosoma* **1979**, *70*, 141–160. [[CrossRef](#)]
21. Berrios, S.; Fernandez-Donoso, R.; Page, J.; Ayarza, E.; Capanna, E.; Solano, E.; Castiglia, R. Hexavalents in spermatocytes of Robertsonian heterozygotes between *Mus m. domesticus* 2n = 26 from the Vulcano and Lipari Islands (Aeolian archipelago, Italy). *Eur. J. Histochem.* **2018**, *62*, 2894. [[CrossRef](#)]
22. Ribagorda, M.; Berrios, S.; Solano, E.; Ayarza, E.; Martín-Ruiz, M.; Gil-Fernández, A.; Parra, M.T.; Viera, A.; Rufas, J.S.; Capanna, E.; et al. Meiotic behavior of a complex hexavalent in heterozygous mice for Robertsonian translocations: Insights for synapsis dynamics. *Chromosoma* **2019**, *128*, 149–163. [[CrossRef](#)]
23. Bogdanov, Y.F.; Kolomiets, O.L.; Lyapunova, E.A.; Yanina, I.Y.; Mazurova, T.F. Synaptonemal complexes and chromosome chains in the rodent *Ellobius talpinus* heterozygous for ten Robertsonian translocations. *Chromosoma* **1986**, *94*, 94–102. [[CrossRef](#)]
24. Matveevsky, S.; Tretiakov, A.; Kashintsova, A.; Bakloushinskaya, I.; Kolomiets, O. Meiotic nuclear architecture in distinct mole vole hybrids with Robertsonian translocations: Chromosome chains, stretched centromeres, and distorted recombination. *Int. J. Mol. Sci.* **2020**, *21*, 7630. [[CrossRef](#)]
25. Merico, V.; Giménez, M.D.; Vasco, C.; Zuccotti, M.; Searle, J.B.; Hauffe, H.C.; Garagna, S. Chromosomal speciation in mice: A cytogenetic analysis of recombination. *Chromosome Res.* **2013**, *21*, 523–533. [[CrossRef](#)]
26. Berrios, S.; Manieu, C.; López-Fenner, J.; Ayarza, E.; Page, J.; González, M.; Manterola, M.; Fernández-Donoso, R. Robertsonian chromosomes and the nuclear architecture of mouse meiotic prophase spermatocytes. *Biol. Res.* **2014**, *47*, 16. [[CrossRef](#)] [[PubMed](#)]
27. Vara, C.; Paytuví-Gallart, A.; Cuartero, Y.; Álvarez-González, L.; Marín-Gual, L.; Garcia, F.; Florit-Sabater, B.; Capilla, L.; Sánchez-Guillén, R.A.; Sarrate, Z.; et al. The impact of chromosomal fusions on 3D genome folding and recombination in the germ line. *Nat. Commun.* **2021**, *12*, 2981. [[CrossRef](#)] [[PubMed](#)]

28. Bakloushinskaya, I.Y.; Romanenko, S.A.; Graphodatsky, A.S.; Matveevsky, S.N.; Lyapunova, E.A.; Kolomiets, O.L. The role of chromosome rearrangements in the evolution of mole voles of the genus *Ellobius* (Rodentia, Mammalia). *Russ. J. Genet.* **2010**, *46*, 1143–1145. [[CrossRef](#)]
29. Matveevsky, S.; Bakloushinskaya, I.; Tambovtseva, V.; Romanenko, S.; Kolomiets, O. Analysis of meiotic chromosome structure and behavior in Robertsonian heterozygotes of *Ellobius tancrei* (Rodentia, Cricetidae): A case of monobrachial homology. *Comp. Cytogenet.* **2015**, *9*, 691. [[CrossRef](#)] [[PubMed](#)]
30. Nunes, A.C.; Catalan, J.; Lopez, J.; Ramalhinho, M.G.; Mathias, M.L.; Britton-Davidian, J. Fertility assessment in hybrids between monobrachially homologous Rb races of the house mouse from the island of Madeira: Implications for modes of chromosomal evolution. *Heredity* **2011**, *106*, 348–356. [[CrossRef](#)]
31. Kolomiets, O.L.; Vorontsov, N.N.; Lyapunova, E.A.; Mazurova, T.F. Ultrastructure, meiotic behavior, and evolution of sex chromosomes of the genus *Ellobius*. *Genetica* **1991**, *84*, 179–189. [[CrossRef](#)]
32. Kolomiets, O.; Matveevsky, S.; Bakloushinskaya, I. Sexual dimorphism in prophase I of meiosis in the Northern mole vole (*Ellobius talpinus Pallas*, 1770) with isomorphic (XX) chromosomes in males and females. *Comp. Cytogenet.* **2010**, *4*, 55–66. [[CrossRef](#)]
33. Matveevsky, S.; Bakloushinskaya, I.; Kolomiets, O. Unique sex chromosome systems in *Ellobius*: How do male XX chromosomes recombine and undergo pachytene chromatin inactivation? *Sci. Rep.* **2016**, *6*, 29949. [[CrossRef](#)]
34. Gil-Fernández, A.; Matveevsky, S.; Martín-Ruiz, M.; Ribagorda, M.; Parra, M.T.; Viera, A.; Rufas, J.S.; Kolomiets, O.; Bakloushinskaya, I.; Page, J. Sex differences in the meiotic behavior of an XX sex chromosome pair in males and females of the mole vole *Ellobius tancrei*: Turning an X into a Y chromosome? *Chromosoma* **2021**, *130*, 113–131. [[CrossRef](#)]
35. Tambovtseva, V.G.; Matveevsky, S.N.; Kashintsova, A.A.; Tretiakov, A.V.; Kolomiets, O.L.; Bakloushinskaya, I.Y. A meiotic mystery in experimental hybrids of the eastern mole vole (*Ellobius tancrei*, Mammalia, Rodentia). *Vavilov J. Genet. Breed.* **2019**, *23*, 239–243. [[CrossRef](#)]
36. Burgoyne, P.S.; Mahadevaiah, S.K.; Turner, J.M. The consequences of asynapsis for mammalian meiosis. *Nat. Rev. Genet.* **2009**, *10*, 207–216. [[CrossRef](#)]
37. Bergero, R.; Ellis, P.; Haerty, W.; Larcombe, L.; Macaulay, I.; Mehta, T.; Mogensen, M.; Murray, D.; Nash, W.; Neale, M.J.; et al. Meiosis and beyond—understanding the mechanistic and evolutionary processes shaping the germline genome. *Biol. Rev.* **2021**, *96*, 822–841. [[CrossRef](#)]
38. Ford, C.E.; Hamerton, J.L. A colchicine, hypotonic citrate, squash sequence for mammalian chromosomes. *Stain Technol.* **1956**, *31*, 247–251. [[CrossRef](#)]
39. Seabright, M. A rapid banding technique for human chromosomes. *Lancet* **1971**, *2*, 971–972. [[CrossRef](#)]
40. Navarro, J.; Vidal, F.; Guitart, M.; Egozcue, J. A method for the sequential study of synaptonemal complexes by light and electron microscopy. *Hum. Genet.* **1981**, *59*, 419–421. [[CrossRef](#)]
41. Schimenti, J. Synapsis or silence. *Nat. Genet.* **2005**, *37*, 11–13. [[CrossRef](#)]
42. Bolcun-Filas, E.; Handel, M.A. Meiosis: The chromosomal foundation of reproduction. *Biol. Reprod.* **2018**, *99*, 112–126. [[CrossRef](#)]
43. Zickler, D.; Kleckner, N. Recombination, pairing, and synapsis of homologs during meiosis. *Cold Spring Harb. Perspect. Biol.* **2015**, *7*, a016626. [[CrossRef](#)]
44. Wang, M.; Zeng, L.; Su, P.; Ma, L.; Zhang, M.; Zhang, Y.Z. Autophagy: A multifaceted player in the fate of sperm. *Hum. Reprod. Update* **2022**, *28*, 200–231. [[CrossRef](#)]
45. Ayarza, E.; González, M.; López, F.; Fernández-Donoso, R.; Page, J.; Berrios, S. Alterations in chromosomal synapses and DNA repair in apoptotic spermatocytes of *Mus m. domesticus*. *Eur. J. Histochem.* **2016**, *60*, 2677. [[CrossRef](#)]
46. Faisal, I.; Kauppi, L. Sex chromosome recombination failure, apoptosis, and fertility in male mice. *Chromosoma* **2016**, *125*, 227–235. [[CrossRef](#)] [[PubMed](#)]
47. Redi, C.A.; Garagna, S.; Hilscher, B.; Winking, H. The effects of some Robertsonian chromosome combinations on the seminiferous epithelium of the mouse. *J. Embryol. Exp. Morphol.* **1985**, *85*, 1–19. [[CrossRef](#)] [[PubMed](#)]
48. Wallace, B.M.; Searle, J.B.; Everett, C.A. Male meiosis and gametogenesis in wild house mice (*Mus musculus domesticus*) from a chromosomal hybrid zone; a comparison between “simple” Robertsonian heterozygotes and homozygotes. *Cytogenet. Cell Genet.* **1992**, *61*, 211–220. [[CrossRef](#)] [[PubMed](#)]
49. Wallace, B.M.; Searle, J.B.; Everett, C.A. The effect of multiple simple Robertsonian heterozygosity on chromosome pairing and fertility of wild-stock house mice (*Mus musculus domesticus*). *Cytogenet. Genome Res.* **2002**, *96*, 276–286. [[CrossRef](#)]
50. Winking, H.; Reuter, C.; Bostelmann, H. Unequal nondisjunction frequencies of trivalent chromosomes in male mice heterozygous for two Robertsonian translocations. *Cytogenet. Genome Res.* **2000**, *91*, 303–306. [[CrossRef](#)]
51. Matveevsky, S.; Kolomiets, O.; Bogdanov, A.; Hakhverdyan, M.; Bakloushinskaya, I. Chromosomal evolution in mole voles *Ellobius* (Cricetidae, Rodentia): Bizarre sex chromosomes, variable autosomes and meiosis. *Genes* **2017**, *8*, 306. [[CrossRef](#)]
52. Turner, J.M.; Mahadevaiah, S.K.; Fernandez-Capetillo, O.; Nussenzweig, A.; Xu, X.; Deng, C.X.; Burgoyne, P.S. Silencing of unsynapsed meiotic chromosomes in the mouse. *Nat. Genet.* **2005**, *37*, 41–47. [[CrossRef](#)]
53. Turner, J.M.; Mahadevaiah, S.K.; Ellis, P.J.; Mitchell, M.J.; Burgoyne, P.S. Pachytene asynapsis drives meiotic sex chromosome inactivation and leads to substantial postmeiotic repression in spermatids. *Dev. Cell* **2006**, *10*, 521–529. [[CrossRef](#)]
54. Homolka, D.; Ivanek, R.; Capkova, J.; Jansa, P.; Forejt, J. Chromosomal rearrangement interferes with meiotic X chromosome inactivation. *Genome Res.* **2007**, *17*, 1431–1437. [[CrossRef](#)]

55. Manterola, M.; Page, J.; Vasco, C.; Berríos, S.; Parra, M.T.; Viera, A.; Rufas, J.S.; Zuccotti, M.; Garagna, S.; Fernández-Donoso, R. A high incidence of meiotic silencing of unsynapsed chromatin is not associated with substantial pachytene loss in heterozygous male mice carrying multiple simple robertsonian translocations. *PLoS Genet.* **2009**, *5*, e1000625. [[CrossRef](#)]
56. Berríos, S.; Fernández-Donoso, R.; Ayarza, E. Synaptic configuration of quadrivalents and their association with the XY bivalent in spermatocytes of Robertsonian heterozygotes of *Mus domesticus*. *Biol. Res.* **2017**, *50*, 38. [[CrossRef](#)]
57. Spangenberg, V.; Losev, M.; Volkhin, I.; Smirnova, S.; Nikitin, P.; Kolomiets, O. DNA environment of centromeres and non-homologous chromosomes interactions in mouse. *Cells* **2021**, *10*, 3375. [[CrossRef](#)]
58. Scherthan, H. A bouquet makes ends meet. *Nat. Rev. Mol. Cell Biol.* **2001**, *2*, 621–627. [[CrossRef](#)]
59. Harper, L.; Golubovskaya, I.; Cande, W.Z. A bouquet of chromosomes. *J. Cell Sci.* **2004**, *117*, 4025–4032. [[CrossRef](#)]
60. Castiglia, R.; Capanna, E. Contact zone between chromosomal races of *Mus musculus domesticus*. 2. Fertility and segregation in laboratory-reared and wild mice heterozygous for multiple Robertsonian rearrangements. *Heredity* **2000**, *85*, 147–156. [[CrossRef](#)]
61. Mayr, E. *Animal Species and Evolution*; Belknap Press of Harvard University Press: Cambridge, MA, USA, 1963.
62. Mayr, E. *The Growth of Biological Thought: Diversity, Evolution, and Inheritance*; Harvard University Press: Cambridge, MA, USA, 1982.
63. Mallet, J. Species, concepts of. In *Encyclopedia of Biodiversity*; Levin, S.A., Ed.; Elsevier: Oxford, UK, 2001; Volume 5, pp. 427–440.
64. Rieseberg, L.H. Hybrid origins of plant species. *Annu. Rev. Ecol. Syst.* **1997**, *28*, 359–389. [[CrossRef](#)]
65. Navarro, A.; Barton, N.H. Accumulating postzygotic isolation genes in parapatry: A new twist on chromosomal speciation. *Evolution* **2003**, *57*, 447–459. [[CrossRef](#)]
66. Lukhtanov, V.A.; Shapoval, N.A.; Anokhin, B.A.; Saifitdinova, A.F.; Kuznetsova, V.G. Homoploid hybrid speciation and genome evolution via chromosome sorting. *Proc. R. Soc. B Biol. Sci.* **2015**, *282*, 20150157. [[CrossRef](#)]
67. Coughlan, J.M.; Matute, D.R. The importance of intrinsic postzygotic barriers throughout the speciation process. *Philos. Trans. R. Soc. B* **2020**, *375*, 20190533. [[CrossRef](#)]
68. Franchini, P.; Kautt, A.F.; Nater, A.; Antonini, G.; Castiglia, R.; Meyer, A.; Solano, E. Reconstructing the evolutionary history of chromosomal races on islands: A genome-wide analysis of natural house mouse populations. *Mol. Biol. Evol.* **2020**, *37*, 2825–2837. [[CrossRef](#)]
69. Potter, S.; Bragg, J.G.; Turakulov, R.; Eldridge, M.D.; Deakin, J.; Kirkpatrick, M.; Edwards, R.J.; Moritz, C. Limited introgression between rock-wallabies with extensive chromosomal rearrangements. *Mol. Biol. Evol.* **2022**, *39*, msab333. [[CrossRef](#)] [[PubMed](#)]
70. Barton, N.H.; Hewitt, G.M. Adaptation, speciation and hybrid zones. *Nature* **1989**, *341*, 497–503. [[CrossRef](#)] [[PubMed](#)]
71. Barton, N.H. On the completion of speciation. *Phil. Trans. R. Soc. B* **2020**, *375*, 20190530. [[CrossRef](#)] [[PubMed](#)]
72. Westram, A.M.; Stankowski, S.; Surendranadh, P.; Barton, N. What is reproductive isolation? *J. Evol. Biol.* **2022**, *35*, 1143–1164. [[CrossRef](#)]
73. Bazykin, A.D. Hypothetical mechanism of speciation. *Evolution* **1969**, *23*, 685–687. [[CrossRef](#)]
74. Dagilis, A.J.; Kirkpatrick, M.; Bolnick, D.I. The evolution of hybrid fitness during speciation. *PLoS Genet.* **2019**, *15*, e1008125. [[CrossRef](#)]
75. Xiong, T.; Mallet, J. On the impermanence of species: The collapse of genetic incompatibilities in hybridizing populations. *Evolution* **2022**, *76*, 2498–2512. [[CrossRef](#)]
76. Mallet, J.; Mullen, S.P. Reproductive isolation is a heuristic, not a measure: A commentary on Westram et al., 2022. *J. Evol. Biol.* **2022**, *35*, 1175–1182. [[CrossRef](#)]
77. Yoshida, K.; Rödelberger, C.; Röseler, W.; Riebesell, M.; Sun, S.; Kikuchi, T.; Sommer, R.J. Chromosome fusions repatterned recombination rate and facilitated reproductive isolation during *Pristionchus* nematode speciation. *Nat. Ecol. Evol.* **2023**. [[CrossRef](#)]

Disclaimer/Publisher’s Note: The statements, opinions and data contained in all publications are solely those of the individual author(s) and contributor(s) and not of MDPI and/or the editor(s). MDPI and/or the editor(s) disclaim responsibility for any injury to people or property resulting from any ideas, methods, instructions or products referred to in the content.